JOURNAL OF SOLID STATE CHEMISTRY **22,** 263–271 (1977)

Solid State Properties and Catalytic Behavior of the α- and β-Vanadium Bronzes

D. K. CHAKRABARTY,* DIPAK GUHA, AND A. B. BISWAS

Department of Chemistry, Indian Institute of Technology, Bombay 400 076, India

Received January 31, 1977; in revised form May 4, 1977

Decomposition of isopropanol (IPA) on V_2O_5, $Li_{0.02}V_2O_5$, $Na_{0.02}V_2O_5$, $Na_{0.06}V_2O_5$, $Li_{0.33}V_2O_5$, and $Na_{0.33}V_2O_5$ has been studied in the temperature range 186–300°C. The first four catalysts (α-phase) show predominately dehydration, whereas the last two (β-phase) have comparable dehydration and dehydrogenation activity. Dehydration activity increases with alkali metal concentration within the α-phase, but falls sharply on the β-phase catalysts. This difference is attributed to the different rate determining steps for the reaction on the α- and β-phase catalysts. X-ray and ir spectral data show that the β-phase catalysts are much more stable than the α-phase. A mechanism for the dehydration of IPA based on the electrical resistivity, ESR spectra, and kinetic data has been proposed.

Introduction

Vanadium forms a series of compounds of the general formula $M_xV_2O_5$, commonly known as vanadium bronzes where M is an alkali metal. Depending upon the value of x, several structural forms have been identified. The α-bronze is isostructural with V_2O_5, which is orthorhombic and the β-bronze has a monoclinic form. The limits of x for the two phases for the lithium and sodium bronzes have been reported to be as follows (*1*):

Compound	α-phase	β-phase
$Li_xV_2O_5$	$0 \leqslant x \leqslant 0.13$	$0.22 \leqslant x \leqslant 0.62$
$Na_xV_2O_5$	$0 \leqslant x \leqslant 0.02$	$0.22 \leqslant x \leqslant 0.40$

Structures of these compounds have been investigated thoroughly (*1–5*). Electrical properties of the α-bronzes have been studied by Chakrabarty et al. (*6*), and that of β-bronzes by several other authors (*3, 7–9*). They are all known to be hopping-type semiconductors, the conduction being due to the jump of electrons from V^{4+} to V^{5+} sites. The V^{4+} sites are created by the trapping of electrons through the ionization of the alkali metal. It has been shown from Hall coefficient measurements (*8*) as well as from ESR studies that each alkali metal atom in the β-bronzes give rise to one V^{4+}, whereas in the α-bronzes the electrons are initially trapped possibly at oxygen defects (*6, 11*). However, the electrons are to be initially excited thermally from the trapping centers to form the V^{4+} site so that it can hop to an adjacent V^{5+} site. Even vanadium pentoxide is a hopping semiconductor, in which V^{4+} centers are present due to nonstoichiometry.

Vanadium pentoxide is an important industrial catalyst, to which alkali salts are often added as promoters. Although the literature is abound with reports on the promoter action of the alkali metals on V_2O_5 catalysts, all of them are concerned with systems containing a large excess of alkali metal, but no report apparently exists on the catalytic activity of the vanadium bronzes. This prompted us to undertake a systematic study of the catalytic properties of

---

* Author to whom all correspondence should be addressed.

ISSN 0022–4596

these compounds. Some preliminary results on the catalytic properties of the lithium vanadium bronzes in the α-phase have been reported by us (*12*). The present paper reports the catalytic decomposition of a model compound, isopropanol (IPA), on the lithium and sodium vanadium bronzes (Both α- and β-phases). A mechanism for the dehydration and dehydrogenation has been suggested based on kinetic data as well as the electrical and spectral properties of the system: catalyst–reactant.

Experimental Methods

The preparation of the bronzes has been reported elsewhere (*6*). The following catalysts were used in this study: V_2O_5, $Li_{0.02}V_2O_5$, $Na_{0.02}V_2O_5$, $Na_{0.06}V_2O_5$ (all in the α-phase) and the two β-bronzes $Li_{0.33}V_2O_5$ and $Na_{0.33}V_2O_5$.

X-ray powder diffractograms were recorded on a Philips PW 1051 diffractometer using CuKα radiation. Ir spectra in nujol were recorded on a Perkin–Elmer model 237 B spectrometer. ESR spectral measurements were carried out on an X-band superheterodyne spectrometer at room temperature using DPPH as the g marker. The samples for ESR were prepared as follows. Equal amounts of the catalysts were taken in sample tubes and evacuated at 10^{-4} Torr, sealed, and the spectra were recorded at room temperature. For taking the ESR spectra after IPA adsorption, IPA was introduced into the evacuated tube containing the catalyst at 60 Torr at room temperature or at 200°C and then sealed.

The method for the measurement of electrical resistivity of the catalysts under the reaction conditions has been described (*13*). The specific surface area of the catalysts was measured by the BET nitrogen adsorption method at the boiling point of nitrogen. Ammonia chemisorption was measured by the volumetric method.

The kinetics of IPA decomposition were studied in a flow reactor 35-cm long and 1.5-cm i.d. in which 1 g of the catalyst was held between glass wool plugs. The temperature of the catalyst was maintained within ±1°C using a chromel–alumel thermocouple as the sensor that was placed inside a glass tube embedded in the catalyst. A steady supply of the reactant was maintained by an arrangement similar to that described by Griffith et al. (*14*). The liquid products were collected in an ice-cooled trap and analyzed by vapor-phase chromatography on an AIMIL Mark II dual column TC dual detector gas chromatograph using carbowax 20M on a chromosorb column employing hydrogen carrier gas. The gaseous products were analyzed by the Orsat method.

Before each run the catalyst was activated by passing dry air for 4 hr at 400°C. After attaining steady state, the activity of pure V_2O_5 and the α-bronzes remained unchanged for about half an hour, but the β-bronzes showed much higher stability.

IPA undergoes both dehydration to give propene and dehydrogenation to acetone. Initial rates (r_i) of the reactions were obtained plotting the moles of water (or acetone) formed per 100 moles of IPA fed against contact time. The energy of activation (E_a) and the preexponential factor (k_0) of these reactions on the various catalysts were obtained.

Results

Ir spectra of V_2O_5, $Na_{0.06}V_2O_5$, $Li_{0.33}V_2O_5$, $Na_{0.33}V_2O_5$ before and after catalysis are shown Fig. 1 as typical representative of the α- and β-phase. V_2O_5 shows a sharp absorption band at 1012 cm^{-1} and a broad band at 820 cm^{-1} which are slightly lower than those reported in the earlier literature (*14*, *15*), but are in very good agreement with the data recently reported (*23*). The spectra of the bronzes are reported here for the first time. It can be seen that the spectra of the α-bronzes are identical with those of V_2O_5, whereas in the β-bronzes the band at 820 cm^{-1} is absent and that at 1012 cm^{-1} is split. The 1012 cm^{-1} band of V_2O_5 has been assigned to the terminal V=O stretching and that at 820

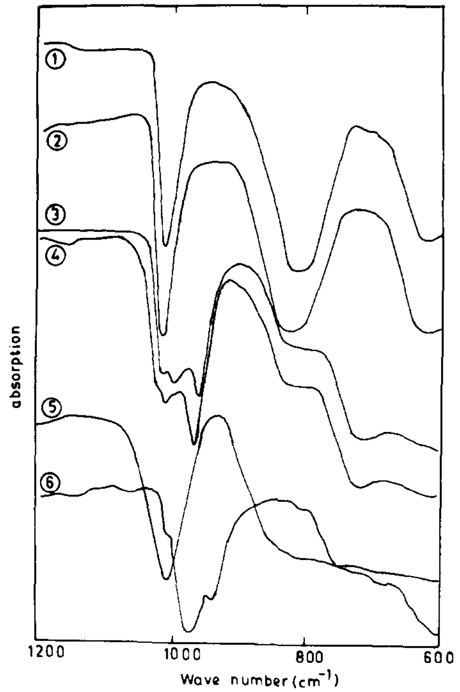

FIG. 1. Ir spectra of the samples before and after catalysis: (1) V_2O_5, (2) $Na_{0.06}V_2O_5$, (3) $Li_{0.33}V_2O_5$, (4) $Na_{0.33}V_2O_5$, (5) V_2O_5 after catalysis, (6) $Na_{0.33}V_2O_5$ after catalysis.

cm^{-1} to the V–O–V stretching. In V_2O_5, all the vanadium atoms have identical oxygen environments, but in β-bronzes there are three different types of vanadium atoms. This possibly is the cause of the splitting of the band near 1012 cm^{-1}. The V–O–V chains in the β-bronzes are characterized by several different V–O distances leading to the complications in the ir spectrum. The spectra of V_2O_5 and the α-bronzes after catalysis show a drastic change in the 820-cm^{-1} region showing that it is the V–O–V chain which is most affected. The spectra of the β-bronzes after catalysis do not show such changes, although the relative intensity of the bands around 1000 cm^{-1} undergoes some modification. This suggests that the β-phase catalysts are much more stable. This conclusion is supported by the X-ray diffractograms of the α- and β-phase catalysts taken before and after the reaction. Figure 2 shows that the structure of $Na_{0.33}V_2O_5$ remains practically unchanged while that of V_2O_5 is greatly changed after its use in the catalytic reaction. The higher stability of the β-bronzes was also observed during kinetic studies.

At room temperature pure V_2O_5 shows an ESR signal at $g = 1.96$ assigned to V^{4+}. Intensity of this signal increases with the increasing concentration of the alkali metal in the bronzes. ESR spectra of V_2O_5 and $Na_{0.06}V_2O_5$ before and after IPA adsorption are presented in Fig. 3. The concentration of V^{4+} increases by IPA adsorption at 200°C as

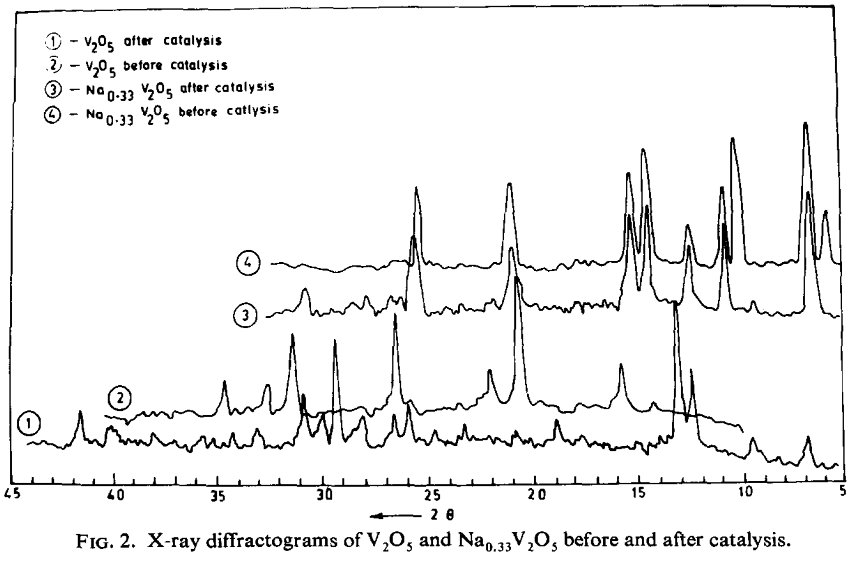

FIG. 2. X-ray diffractograms of V_2O_5 and $Na_{0.33}V_2O_5$ before and after catalysis.

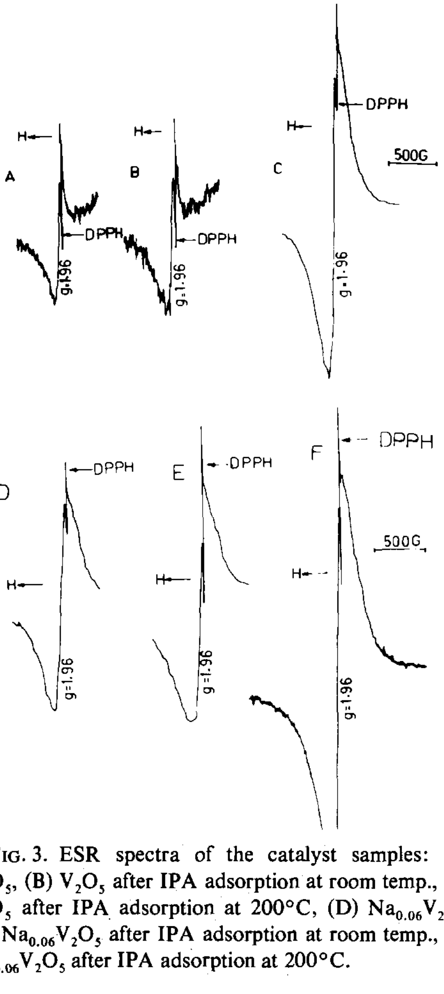

FIG. 3. ESR spectra of the catalyst samples: (A) V_2O_5, (B) V_2O_5 after IPA adsorption at room temp., (C) V_2O_5 after IPA adsorption at 200°C, (D) $Na_{0.06}V_2O_5$, (E) $Na_{0.06}V_2O_5$ after IPA adsorption at room temp., (F) $Na_{0.06}V_2O_5$ after IPA adsorption at 200°C.

TABLE I

DEHYDRATION OF ISOPROPANOL ON THE α-VANADIUM BRONZES

Catalyst	Surface area (m^2/g)	k_0 (m^{-2} sec^{-1})	E_a (kcal/mole)
V_2O_5	3.1	3.16×10^3	5.07
$Li_{0.02}V_2O_5$	3.0	4.76×10^3	5.06
$Na_{0.02}V_2O_5$	2.9	5.41×10^3	5.06
$Na_{0.06}V_2O_5$	3.0	6.56×10^3	5.06

shown by the ESR spectra. Similar behavior was shown by the other catalysts.

The results of the catalytic decomposition of IPA are presented in Tables I and II. V_2O_5 and the α-bronzes show predominantly dehydration activity and very little dehydrogenation. Formation of small quantities of diisopropyl ether (DIE) has been noticed at lower temperature. An increase in the concentration of alkali metal (within the α-phase range) increases dehydration activity. The increase is due to an increase in the preexponential factor (k_0) as the Arrhenius activation energy (E_a) remains unchanged. The Arrhenius plots are shown in Fig. 4.

The effect of the partial pressure of IPA (p_{IPA}) on its decomposition on V_2O_5 catalyst in the presence of nitrogen, propene, acetone, and water vapor, respectively, is shown in Fig. 5. In these studies, the total pressure was maintained at 1 atm with varying p_{IPA} from 0.6–1 atm and the second component (water, propene, nitrogen, or acetone) added at 0.4, 0.3, 0.2, and 0.1 atm. It can be seen that dehydration is reduced by increasing the partial pressure of water (p_{H_2O}) in the reactant, but is unaffected by the rest. Similarly, dehydrogenation is lowered by increasing the partial pressure of acetone (p_{ac}) only. Similar results are shown by the α-bronzes.

The β-bronzes have comparable dehydration and dehydrogenation activity. The effect of p_{IPA} on dehydration and dehydrogenation on $Na_{0.33}V_2O_5$ is shown in Fig. 6.

TABLE II

DECOMPOSITION OF ISOPROPANOL ON THE β-BRONZES

Catalyst	Surface area (m^2/g)	Dehydration		Dehydrogenation	
		k_0 (m^{-2} sec^{-1})	E_a (kcal/mole)	k_0 (m^{-2} sec^{-1})	E_a (kcal/mole)
$Li_{0.33}V_2O_5$	2.8	2.05×10^3	5.01	4.18×10^3	5.7
$Na_{0.33}V_2O_5$	2.7	2.31×10^3	5.0	4.26×10^3	5.5

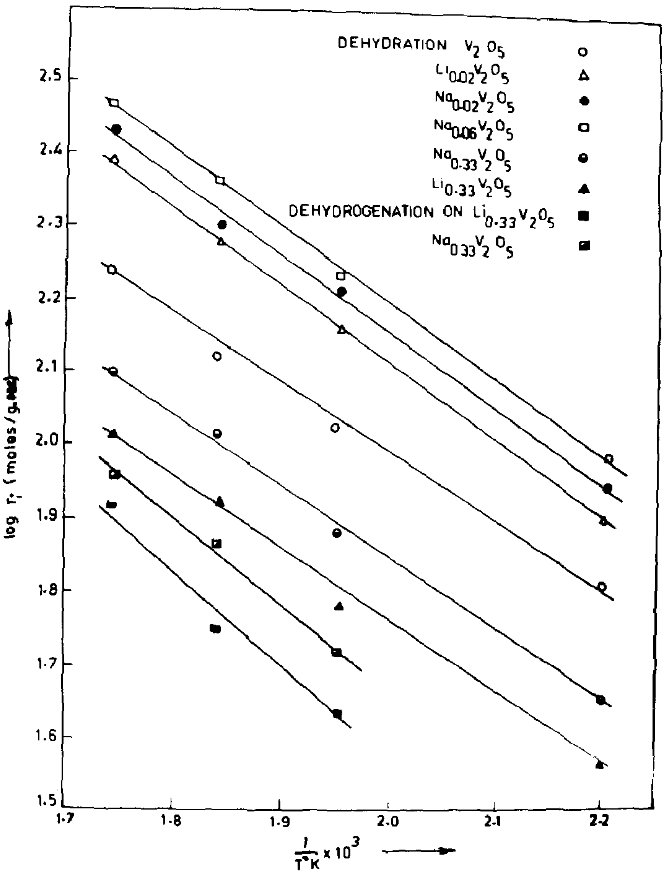

FIG. 4. Arrhenius plots for dehydration and dehydrogenation of IPA on the vanadium bronzes.

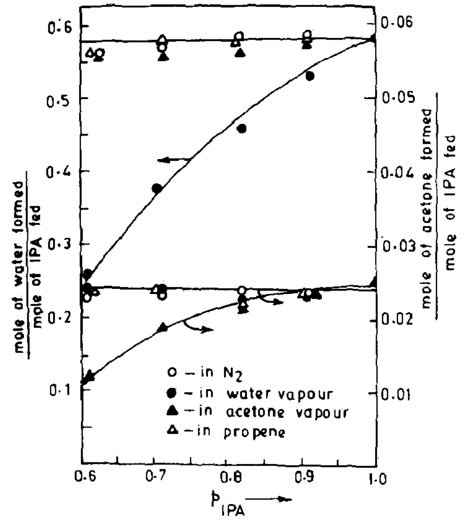

FIG. 5. The effect of the various reaction products on the decomposition of IPA on V_2O_5 (1 g of catalyst; contact time 0.51 sec., temperature 270°C).

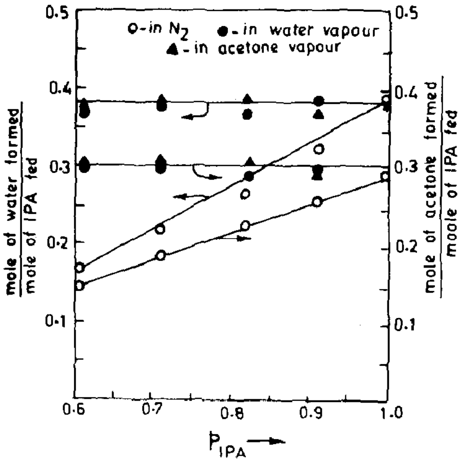

FIG. 6. The effect of the various reaction products on the decomposition of IPA on $Na_{0.33}V_2O_5$ (1 g of catalyst; contact time 0.51 sec.; temperature 270°C).

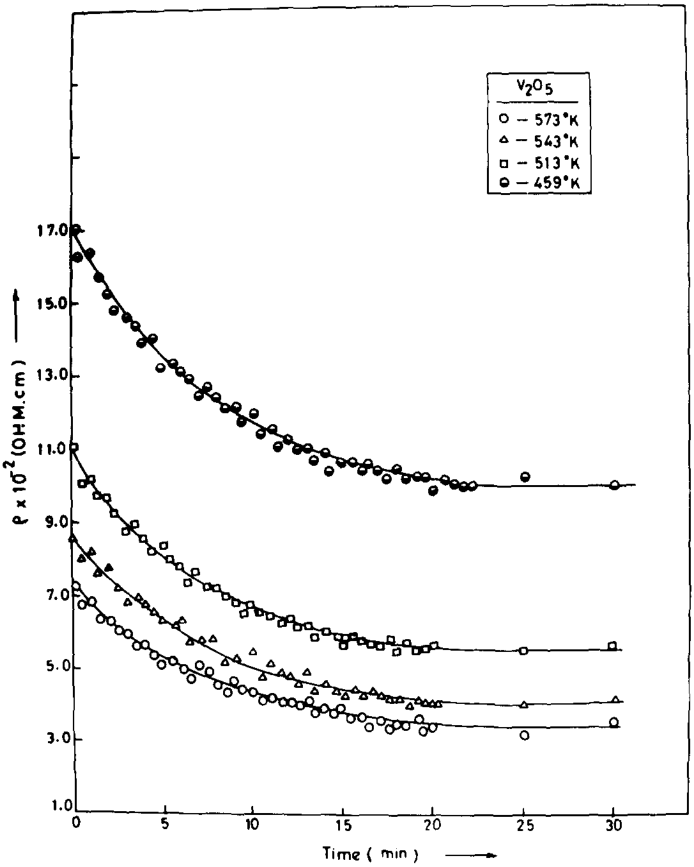

FIG. 7. Change in electrical resistivity of V_2O_5 with time after introducing IPA vapor.

Neither of the reactions are affected by the presence of any of the products including water and acetone.

Electrical resistivity (ρ) of the samples decreases rapidly in the presence of IPA vapor at temperatures above 170°C attaining a constant value in about 15 min. Below this temperature, the presence of IPA vapor does not affect resistivity. Figure 7 shows the resistivity vs time plots for V_2O_5 in the presence of IPA. The other catalysts showed qualitatively similar results. The fall in resistivity (Δ log ρ) was calculated for each temperature and catalyst from initial and final resistivities. Plots of maximum dehydration yield at the corresponding temperature vs Δ log ρ was found to be linear (Fig. 8).

Chemisorption of ammonia on V_2O_5 and $Na_{0.06}V_2O_5$ was measured between 200–300°C. It was found that ammonia adsorbed per unit surface area was higher for $Na_{0.06}V_2O_5$ than for V_2O_5.

Discussions

The specific surface of the catalysts shows a little decrease with increasing alkali metal concentration. Hence the higher dehydration activity of the α-bronzes as compared to pure V_2O_5 cannot be attributed to the change in surface area.

The electrical conductivity data of the pelletized catalysts are revealing. It is well known that pure V_2O_5 and the bronzes are *n*-type semiconductors and conductivity increases with increase of x in $M_xV_2O_5$ (*6*, *17*). In the presence of IPA, conductivity is further enhanced but only at temperatures >170°C.

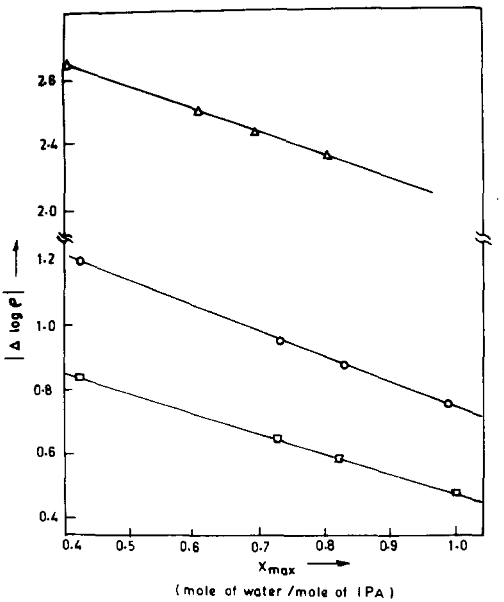

FIG. 8. Δ log ρ vs maximum dehydration yield plots for the various catalysts.

Interestingly, this is the temperature above which noticable decomposition of IPA could occur. Since V_2O_5 and the vanadium bronzes are hopping semiconductors, the increase in conductivity must be due to an increase in V^{4+} concentration. That adsorption of IPA at its decomposition temperature leads to an increase in V^{4+} concentration is evidenced by the enhanced ESR signal at $g = 1.96$. This indicates that V^{4+} concentration increases to a significant extent during IPA decomposition. This can happen due to a dissociative chemisorption of the alcohol. It was suggested by Volkenshtein (*17*) that an alcohol molecule may undergo heterolytic dissociative adsorption as OH^- and an alcohol residue. If now the OH^- is adsorbed on a V^{5+} site, the latter may extract its electron to become V^{4+} as follows:

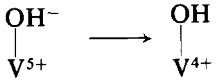

$$\begin{array}{c}\mathrm{OH}^-\\ |\\ \mathrm{V}^{5+}\end{array} \longrightarrow \begin{array}{c}\mathrm{OH}\\ |\\ \mathrm{V}^{4+}\end{array}$$

Next, let us look for the possible rate determining step. As seen from Fig. 5, the dehydration reaction on the α-phase catalyst is dependent on p_{H_2O} and dehydrogenation on p_{ac}; we are inclined to accept that the desorption of water and acetone are the rate controlling steps, although the surface reaction as the slowest step cannot be ruled out. The reactions on the β-bronzes are unaffected by the products, and adsorption of IPA seems to be rate determining (Fig. 6).

It is seen that dehydration is the main reaction on V_2O_5 and the α-bronzes. Dehydration of alcohols has been widely studied on alumina and silica–alumina catalysts. It is generally held that surface acidity (Lewis or Bronsted) is responsible for alcohol dehydration (*18–22*). Since dehydration on the α-bronzes increases with x, Bronsted acidity cannot be responsible for this reaction as the alkali metals will destroy such acidity. However, an increase in ammonia adsorption on the sodium bronzes as compared to that on V_2O_5 indicates that the surface concentration of the Lewis acid centers increases by addition of alkali metals. Since doping with alkali metals also increases V^{4+} concentration, it seems reasonable to assume that ammonia is adsorbed at V^{4+} sites. V^{4+} sites. V^{4+} with a d^1 configuration will be preferred for ammonia coordination due to the gain in crystal field stabilization energy.

Volkenshtein (*17*) has suggested that adsorption of alcohols on a semiconductor surface can take place either by breaking the C–OH or the O–H bond, the first will lead to dehydration and the second to dehydrogenation. He could just as well show that the reaction rate is related to the Fermi energy of the band-type semiconductor which also controls the surface concentration of the different reacting species. It is, however, well known by now that V_2O_5 and the vanadium bronzes are hopping-type semiconductors. The charge carriers are localized and one will have to apply the localized model of semiconduction and catalysis. If we accept that the rupture of the C–OH bond is responsible for dehydration (*17*), we can propose the following tentative mechanism for IPA dehydration. This will explain (1) the increase in electrical conductivity on IPA adsorption, (2) the increase in

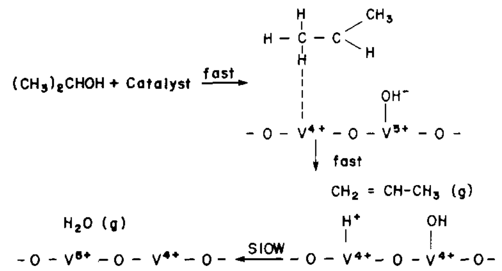

the intensity of the ESR signal on IPA adsorption, (3) the effect of water vapor on dehydration rate, and also (4) the increase in dehydration activity by increasing the concentration of alkali metal, because the slowest step is favored by an increased V^{4+} concentration.

When the V^{4+} concentration is very high (as in the β-bronzes), the water desorption rate increases considerably and ceases to be the rate determining step. The experimental results suggest that IPA adsorption is the slowest step for both the reactions on the β-bronzes. When adsorption is the rate determining step, V^{5+} concentration will determine the rate and since in the β-bronzes V^{4+} concentration is greatly increased as compared to that in the α-bronzes, dehydration activity falls.

Another interesting observation is that the energy of activation for dehydration of IPA is the same in all the samples. The change in the rate is due to the change in the preexponential factor (k_0).

The band theory of catalysis (*17*) relates E_a to Fermi energy. But as mentioned earlier, the electrical properties of these compounds can be explained only by the localized electron model. E_a should then be related to mobility activation energy of the solid, which does not change appreciably from the one sample to another.

The increase in k_0 on increasing alkali metal concentration in the α-bronze is due to increased V^{4+} concentration, which is the active site for dehydration. In the β-bronzes, however, k_0 is small despite a large V^{4+} concentration. This is because of a different rate determining step which needs V^{5+} rather than V^{4+}.

In order to explain the electrical properties of copper-doped V_2O_5 (α-phase), Perlstein (*11*), invoked a dislocation model. According to this, a dislocation structure is created by slippage of the *a–c* plane by 0.2 lattice spacing along the *a*-axis and 0.5 lattice spacing along the *c*-axis. This will create a V–V molecular orbital and an equal number of interstitial oxygen atoms. Perlstein has suggested that such mobile interstitial oxygen atoms, which may be up to 10% of the total oxygen, may have an important bearing on the catalytic property of V_2O_5.

It seems that such mobile oxygen atoms will be easily exchangable with ambient oxygen, and hence should have an important role to play in oxidation reactions. In fact, oxides with high rates of oxygen exchange show only dehydrogenation of alcohols. The α-bronzes, on the other hand, showed only dehydration of IPA. Besides, even if one accepts the dislocation model, at the temperature of dehydration (<300°C) the V–V bond will possibly break up and the interstitial oxygen will take up lattice position. Thus, interstitial oxygen does not seem to be playing an important role in IPA dehydration. It will, however, be interesting to examine simple oxidation reactions, such as CO oxidation where interstitial oxygen is likely to play an important role.

We have demonstrated in this paper that electrical properties of solids can be very helpful in understanding their catalytic activity even when band conduction is absent.

Acknowledgement

The authors express their thanks to Mr. T. Gundu Rao, Physics Department, Indian Insititute of Technology, Bombay, for recording the ESR spectra.

References

1. M. Pouchard, A. Casalot, J. Galy, and P. Hagenmuller, *Bull. Soc. Chim. Fr.* **11**, 4363 (1967).

2. A. D. Wadsley, *Acta Crystallogr.* **8**, 695 (1955).
3. R. P. Ozerov, G. H. Golder, and G. S. Zhdanov, *Sov. Phys. Crystallogr.* **2**, 211 (1957).
4. E. Gillis and E. Boesman, *Phys. Stat. Solidi* **14**, 337 (1966).
5. J. Galy, D. Lavaud, A. Casalot, and P. Hagenmuller, *J. Solid State Chem.* **2**, 531 (1970).
6. D. K. Chakrabarty, D. Guha, and A. B. Biswas, *J. Mater. Sci.* **11**, 1347 (1976).
7. M. Pouchard, A. Casalot, G. Villeneuve, and P. Hagenmuller, *Mater. Res. Bull.* **2**, 877 (1967).
8. J. H. Perlstein and M. J. Sienko, *J. Chem. Phys.* **48**, 174 (1968).
9. A. Casalot and P. Hagenmuller, *J. Phys. Chem. Solids* **30**, 1341 (1969).
10. J. Glendell, R. M. Cotts, and M. J. Sienko, *J. Chem. Phys.* **37**, 220 (1962).
11. J. H. Perlstein, *J. Solid State Chem.* **3**, 217 (1971).
12. D. K. Chakrabarty, D. Guha, I. K. Bhatnagar, and A. B. Biswas, *J. Catalysis* **45**, 305 (1976).
13. D. K. Chakrabarty, K. S. Rane, and A. B. Biswas, *Indian J. Chem.*, to appear.
14. Y. Kera and K. Hirota, *J. Phys. Chem.* **73**, 3973 (1969).
15. G. Fabbri and P. Baraldi, *Anal. Chem.* **44**, 1325 (1972).
16. J. B. Goodenough, *J. Solid State Chem.* **1**, 349 (1970).
17. F. F. Volkenshtein, "Electronic Theory of Catalysis on Semiconductors," Fizmatgiz, Moscow, 1960.
18. H. Knozinger, *J. Catalysis* **12**, 121 (1968).
19. F. Figueras-Roca, L. De Mourgues, and Y. Trambouze, *J. Catalysis* **14**, 107 (1969).
20. F. Figueras-Roca, A. Nohl, L. De Mourgues, and Y. Trambouze, *Trans. Faraday Soc.* **67**, 1155 (1971).
21. K. R. Bakshi and G. R. Gavalas, *J. Catalysis* **38**, 312 (1975).
22. O. V. Krylov, *Zh. Fiz. Khim.* **39**, 2911 (1965).
23. D. J. Cole, C. F. Cullis, and D. J. Hucknall, *JCS Faraday Trans. 1*, **72**, 2185 (1976).